ISSN 1064-2269, Journal of Communications Technology and Electronics, 2016, Vol. 61, No. 7, pp. 776–782. © Pleiades Publishing, Inc., 2016.
Original Russian Text © A.S. Godin, A.I. Kruglov, K.N. Klimov, 2016, published in Radiotekhnika i Elektronika, 2016, Vol. 61, No. 7, pp. 639–645.

ELECTRODYNAMICS AND WAVE PROPAGATION

Numerical Electrodynamic Analysis of the Far-Field Patterns of the External Sestroretskii Cube

A. S. Godin[a], A. I. Kruglov[b], and K. N. Klimov[a]

[a] *Lianozovo Electromechanical Plant Research and Production Corporation, Dmitrovskoe sh. 110, Moscow, 127411 Russia*

[b] *"CADFEM CIS", ul. Suzdal'skaya 46, Moscow, 111672 Russia*

e-mail: andrey.godin@gmail.com, const0@mail.ru

Received October 29, 2014

Abstract—Far-field patterns of the external Sestroretskii cube with the edge size of 1 mm for the frequencies of 1, 150, and 300 GHz are presented. The paradox of the external Sestroretskii cube and its relation to the paradox of the external Huygens cube are revealed.

DOI: 10.1134/S1064226916070056

INTRODUCTION

In [1], the frequency characteristics—SWR, losses, attenuation, and gain—of the external Sestroretskii cube radiating to the free space were numerically simulated and compared with the frequency characteristics of the internal Sestroretskii cube [2]. For estimating the limiting characteristics that can be reached in real radiators, it is also necessary to study the far-field patterns of the external Sestroretskii cube and their frequency dependences. It should be noted that, in contrast to the external Huygens cube [3], the external Sestroretskii cube enables one to simulate the propagation of a plane electromagnetic wave in the directions of three spatial coordinates.

1. STATEMENT OF THE PROBLEM

Let us consider a cube A with the dimensions of $1 \times 1 \times 1$ mm (Fig. 1). The cube A is filled with metal. To each face of the cube A, a rectangular parallelepiped also filled with metal is attached. The bases of the rectangular parallelepipeds coincide with the faces of the cube A and have the same height $h = 0.05$ mm. The number of rectangular parallelepipeds is six, which equals the number of faces of the cube A. Figure 2 shows the faces of rectangular parallelepipeds adjacent to the cube A on which we impose the zero boundary conditions for the tangential component of the electric field, E_τ, which corresponds to a metal wall. These faces will be considered short-circuit (SC) walls [3–5].

Figure 3 shows the faces of the rectangular parallelepipeds attached to the cube A on which we impose the zero boundary conditions for the tangential component of the magnetic field, H_τ, which corresponds to a magnetic wall. These faces will be considered open-circuit (OC) walls [6–8].

On the remaining faces of the rectangular parallelepipeds connected to the cube A (Fig. 4), we impose the boundary conditions of excitation and matching of plane waves [6–8], which correspond to the ports of the Sestroretskii cube. The numeration of the ports is also shown in Fig. 4. The polarizations of the electric and magnetic fields and the directions of the Poynting vectors S [9–12] of the incident plane waves are shown in Fig. 5.

For the consideration of the external electrodynamic problem, let us place the suggested geometry

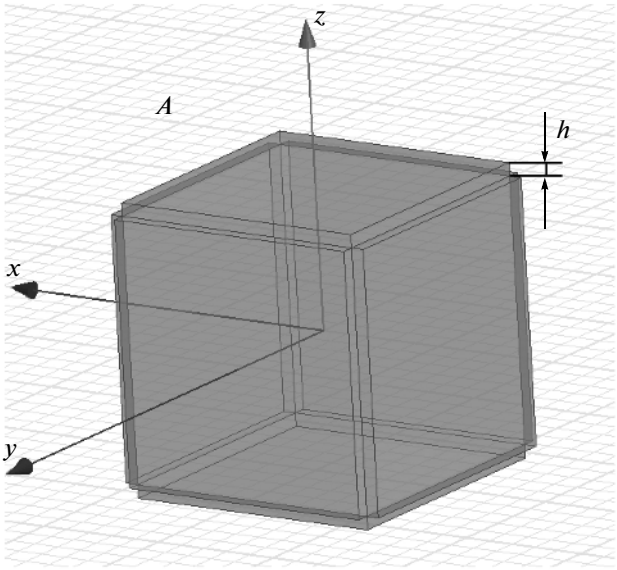

Fig. 1. Geometry of cube A and metal-filled rectangular parallelepipeds attached to its faces.

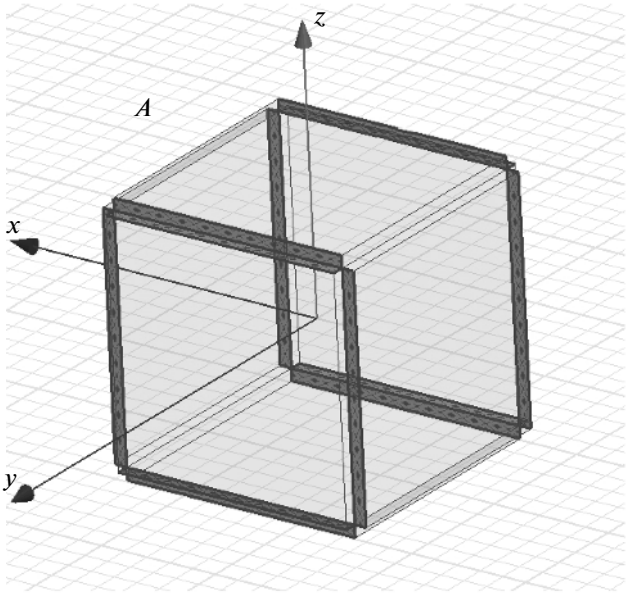

Fig. 2. Faces of rectangular parallelepipeds on which the SC condition is imposed.

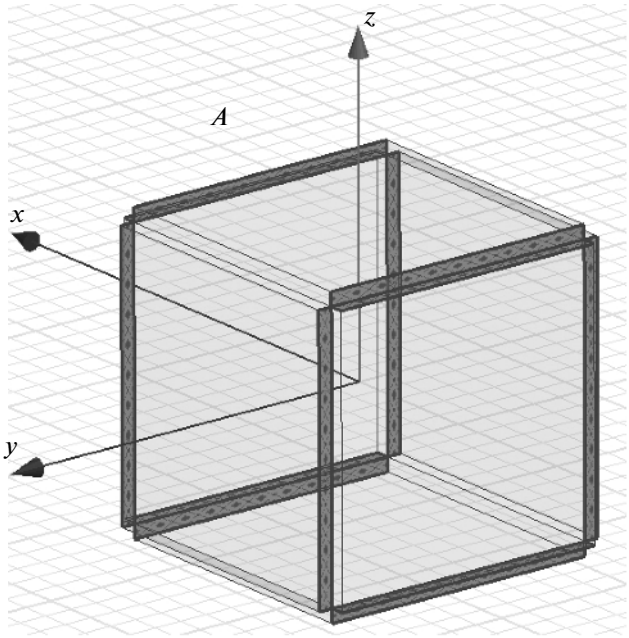

Fig. 3. Faces of rectangular parallelepipeds on which the OC condition is imposed.

with the above boundary conditions into an air cube *B* (Fig. 6), on the faces of which we impose the radiation conditions [13]. The external air cube *B* has the dimensions of $5 \times 5 \times 5$ mm. The cube *B* is filled with vacuum.

Figure 7 shows the faces of the cube *B*, on which the radiation boundary conditions are imposed.

The above geometry of the metal-filled cube *A* together with the six metal-filled rectangular parallelepipeds connected to its faces, all being placed into an air cube *B* with the boundary conditions introduced above, will be called the external Sestroretskii cube.

According to [1], the far-field pattern of the external Sestroretskii cube can be found from the far-field

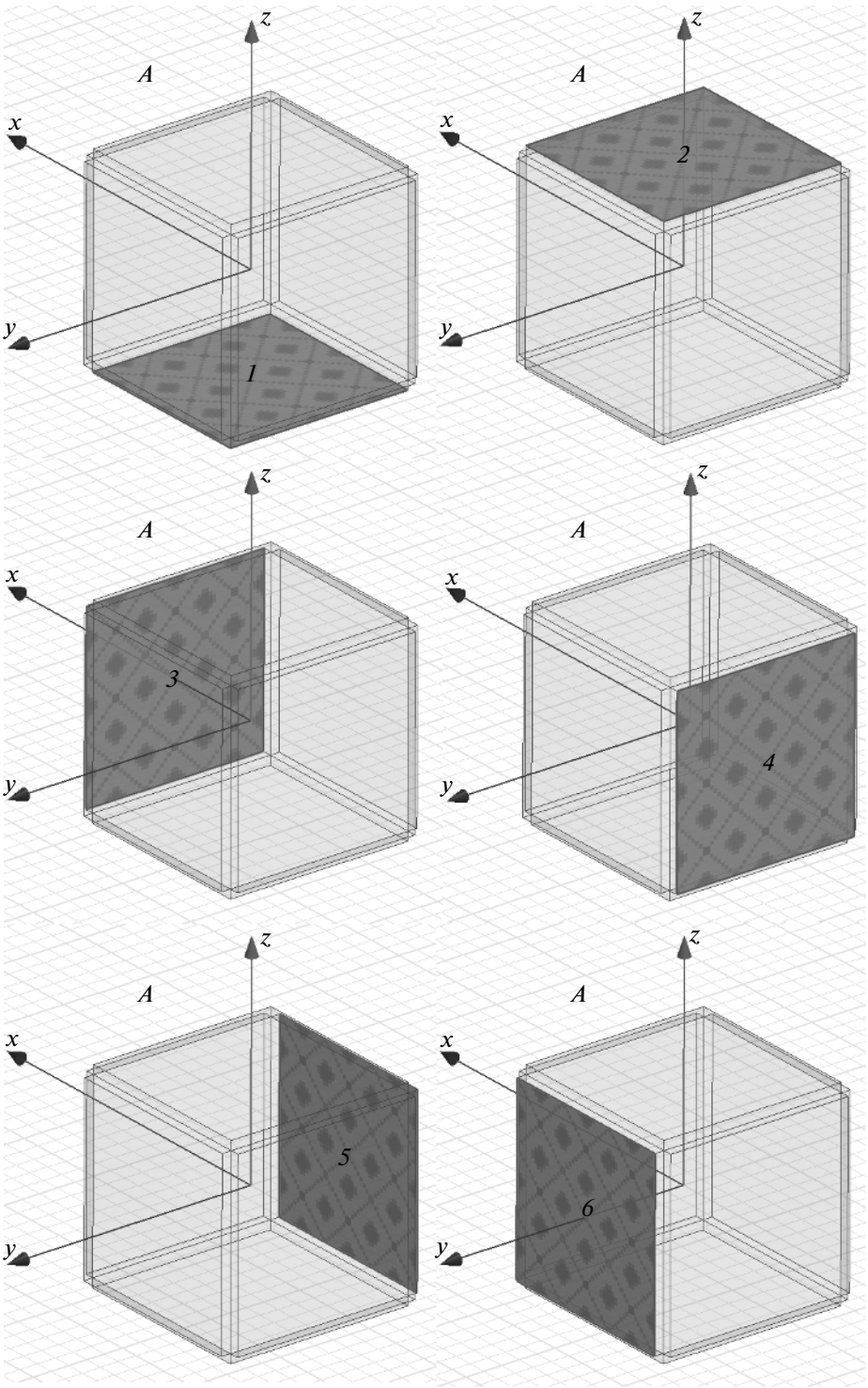

Fig. 4. Faces of rectangular parallelepipeds attached to cube A, on which the conditions of excitation and matching of plane waves are imposed.

patters of the halves of the cube under the in-phase and antiphase excitations.

The far-field patters of a half of the external Sestroretskii cube under in-phase excitation (HESCIE) were calculated in a frequency band of 1 to 300 GHz with a step of 1 GHz. The tolerance for the absolute values of the components of the scattering matrix was Delta $S = 0.02$. The total number of tetrahedra was 28034, and the size of the resulting matrix was 180548, which required 1.17 GB of RAM. The

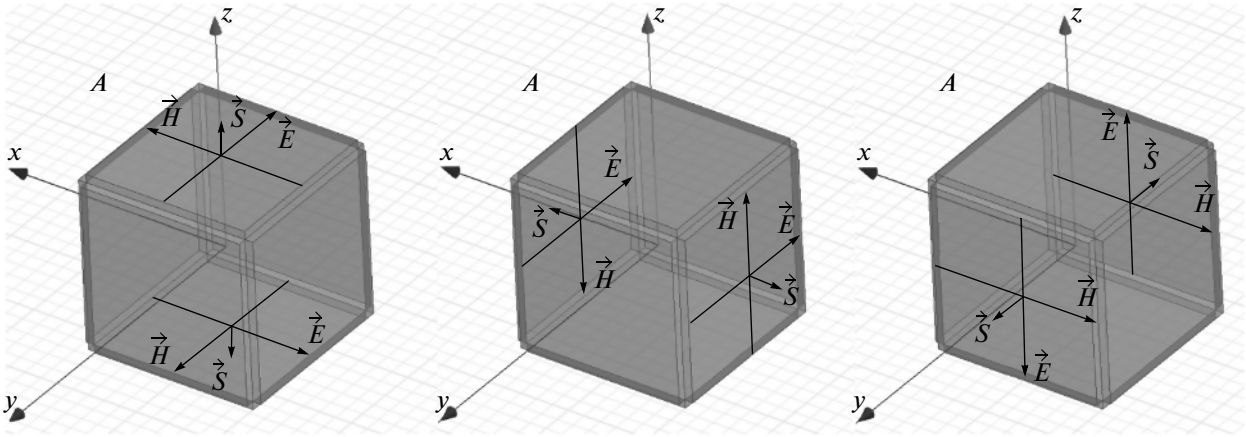

Fig. 5. Direction of the vectors of the electric, $\vec{E}$, and magnetic, $\vec{H}$, fields and the direction of the Poynting vector $\vec{S}$ for the waves incident onto the ports of the external Sestroretskii cube.

total computation time on a PC with an Intel Core i7 2.79 GHz processor and 12 GB RAM was 7 h 19 min 55 s.

Since the geometry of the half of the external Sestroretskii cube under antiphase excitation (HESCAE) is dual [14] to the geometry of the HESCIE on the rotations of the HESCAE about the axis z by 90°, the far-field patterns of the HESCAE can be obtained from the results of calculations for the HESCIE, as it was made in [1].

Let us present the results of the far-field patters of the external Sestroretskii cube from the far-field patterns obtained for the HESCIE and HESCAE.

2. RESULTS OF SIMULATION OF THE FAR-FIELD PATTERNS OF THE EXTERNAL SESTRORETSKII CUBE

Figures 8 and 9 show the characteristics of the 3D far-field patterns for port *2* of the external Sestroretskii cube at a frequency of 1 GHz.

On the excitation of port *2* of the external Sestroretskii cube at the frequency of 1 GHz (see Fig. 8), the far-field pattern has the shape of a cardioid. The direction of maximum radiation coincides with the z-axis. The maximum K_{gain} is –67.26 dB (see Fig. 9). The most part of energy at the frequency of 1 GHz is absorbed at ports *3*, *4*, *5*, and *6* [1]. By analogy with the external Huygens cube [5], this situation

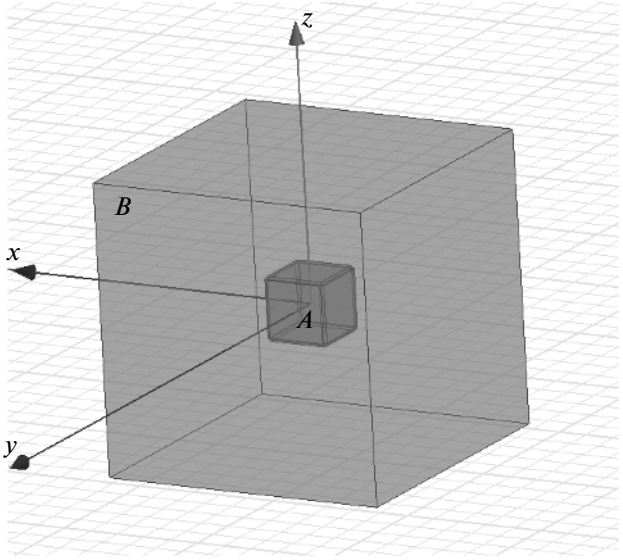

Fig. 6. Geometry of the external electrodynamic problem in the ANSYS HFSS v.15 code.

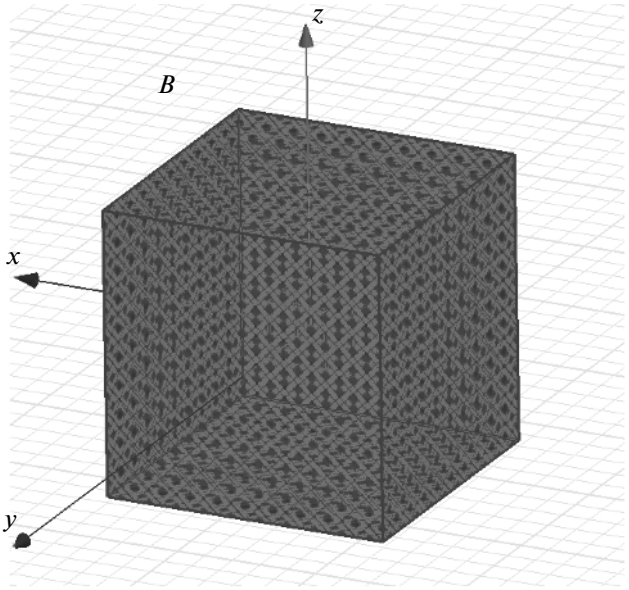

Fig. 7. Radiation boundary conditions on the faces of air cube *B*.

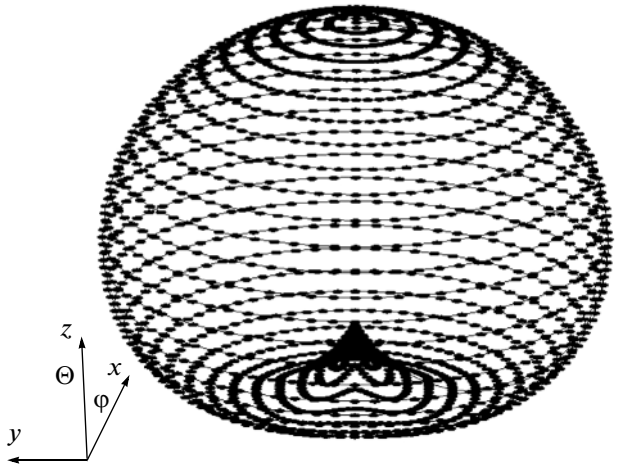

Fig. 8. 3D far-field pattern on the excitation of port *2* of the external Sestroretskii cube at a frequency of 1 GHz.

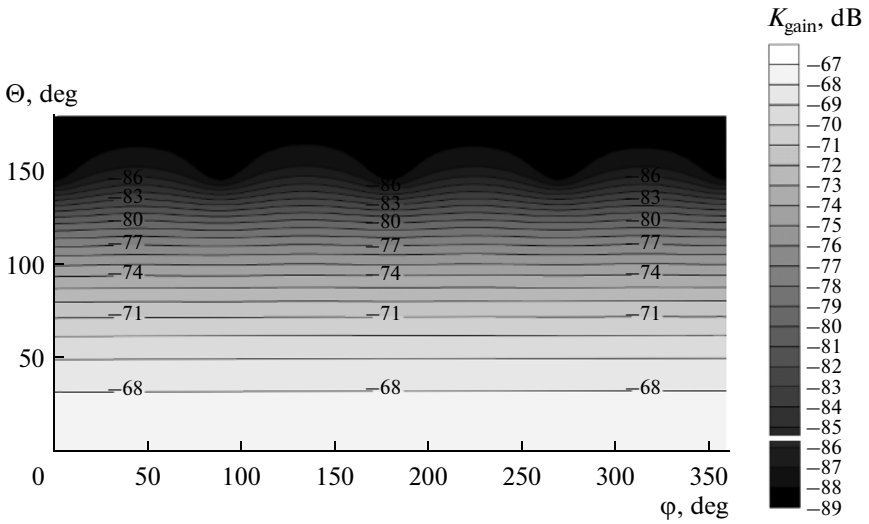

Fig. 9. The cartographic projection of the dependence of K_{gain} on the direction of excitation of port *2* of the external Sestroretskii cube at a frequency of 1 GHz.

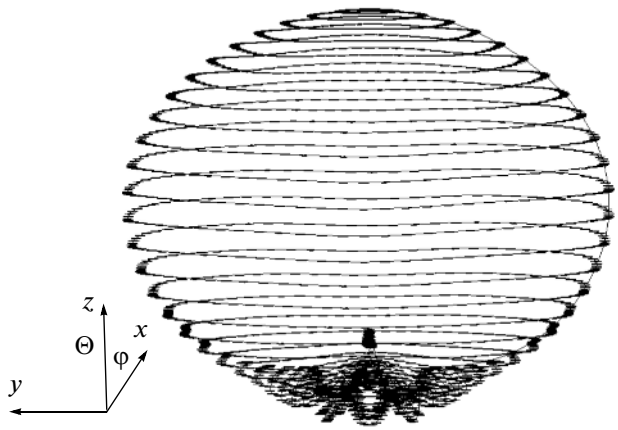

Fig. 10. 3D far-field pattern on the excitation of port *2* of the external Sestroretskii cube at a frequency of 150 GHz.

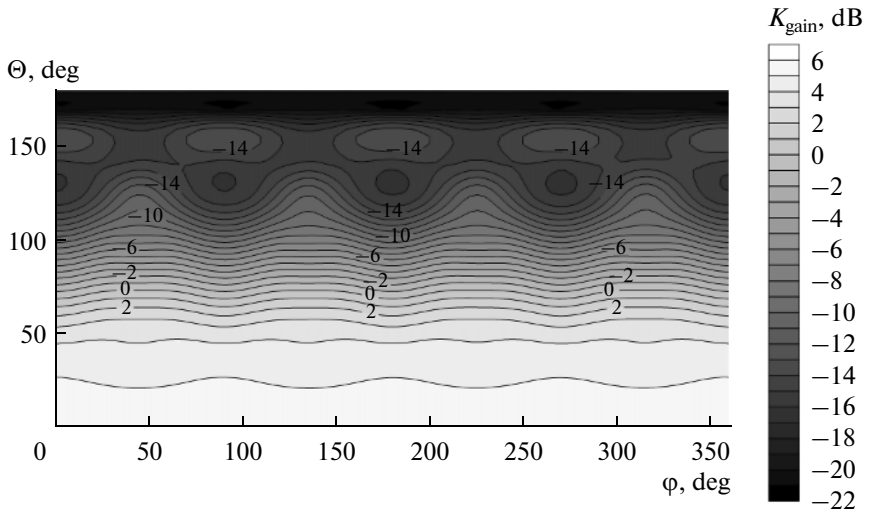

Fig. 11. The cartographic projection of the dependence of K_{gain} on the direction of excitation of port *2* of the external Sestroretskii cube at a frequency of 150 GHz.

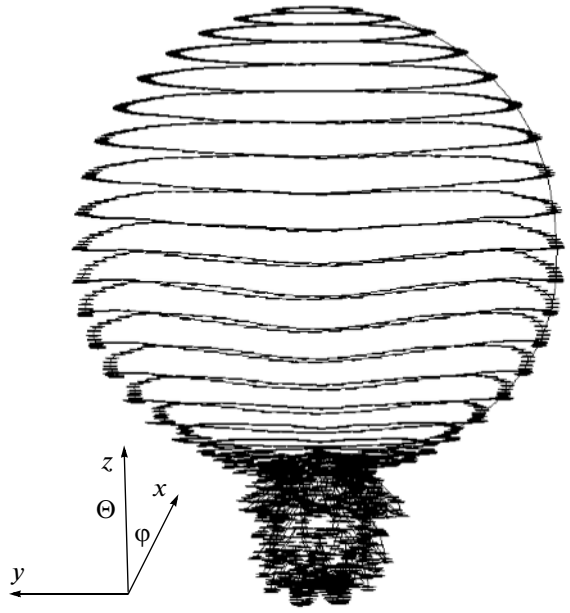

Fig. 12. 3D far-field pattern on the excitation of port *2* of the external Sestroretskii cube at a frequency of 300 GHz.

may be called the paradox of the external Sestroretskii cube: the maximum of the far field is directed along the *z*-axis, but practically all energy is absorbed on the side ports. The external Huygens cube is the external Sestroretskii cube with the OC condition imposed on ports *3* and *4* and the SC condition on ports *5* and *6* [3]. In this case, we may say that the paradox of the external Huygens cube, revealed in [3], is an implication of the aforementioned paradox of the external Sestroretskii cube.

Let us present the 3D far-field pattern of the external Sestroretskii cube on the excitation of port *2* at a frequency of 150 GHz (Fig. 10), which corresponds to the edge length of the external Sestroretskii cube of half the wavelength.

The maximum K_{gain} of the external Sestroretskii cube at a frequency of 150 GHz is 5.5 dB. Figure 11 shows the cartographic projection of the dependence of K_{gain} on the direction of excitation of port *2* of the external Sestroretskii cube at a frequency of 150 GHz.

Now let us present the 3D far-field pattern of the external Sestroretskii cube on the excitation of port *2* at a frequency of 300 GHz (Fig. 12), which corre-

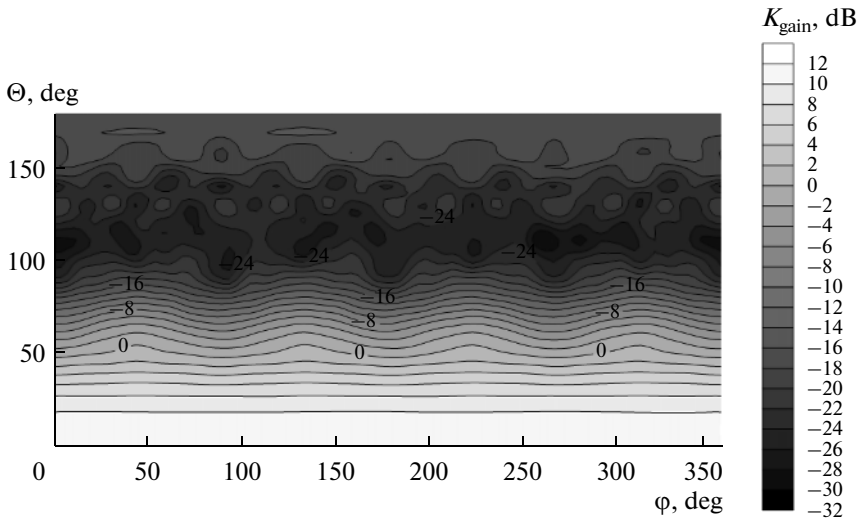

Fig. 13. The cartographic projection of the dependence of K_{gain} on the direction of excitation of port *2* of the external Sestroretskii cube at a frequency of 300 GHz.

sponds to the edge length of the external Sestroretskii cube of one wavelength.

The maximum K_{gain} of the external Sestroretskii cube at a frequency of 300 GHz is 11.82 dB. Figure 13 shows the cartographic projection of the dependence of K_{gain} on the direction of excitation of port *2* of the external Sestroretskii cube at a frequency of 300 GHz.

CONCLUSIONS

Far-field patterns of the external Sestroretskii cube for the frequencies corresponding to the edge length of 1/300 of the wavelength, half-wavelength, and one wavelength are presented. The paradox of the external Sestroretskii cube has been revealed. It is formulated as follows: if the edge length of the external Sestroretskii cube is much smaller than the wavelength, then the direction of the maximum far field and the direction of the main energy flux are mutually orthogonal.

REFERENCES

1. A. S. Godin, M. S. Matsayan, and K. N. Klimov, Radiotekh. Elektron. (Moscow) **61** (5), 401 (2016).
2. A. S. Godin, M. S. Matsayan, and K. N. Klimov, Radiotekh. Elektron. (Moscow) **61** (6), 534 (2016).
3. A. S. Godin, A. B. Tsai, and K. N. Klimov, J. Commun. Technol. Electron. **60**, 436 (2015).
4. A. S. Godin, A. B. Tsai, and K. N. Klimov, J. Commun. Technol. Electron. **60**, 329 (2015).
5. A. S. Godin, A. B. Tsai, and K. N. Klimov, J. Commun. Technol. Electron. **60**, 737 (2015).
6. D. M. Sazonov, A. N. Gridin, and B. A. Mishustin, *Microwave Circuits* (Vysshaya Shkola, Moscow, 1981; Mir, Moscow, 1982).
7. K. N. Klimov, D. S. Gezha, and D. O. Firsov-Shibaev, *Practical Application of Electrodynamic Modeling* (Lambert Academic Publishing, Saarbrücken, 2012) [in Russian].
8. K. N. Klimov, D. O. Firsov-Shibaev, and D. S. Gezha, *Method of Impedance Analysis of Electromagnetic Space* (Lambert Academic Publishing, Saarbrücken, 2013) [in Russian].
9. G. T. Markov and D. M. Sazonov, *Antennas* (Energiya, Moscow, 1975) [in Russian].
10. S. I. Baskakov, *Fundamentals of Electrodynamics* (Sovetskoe Radio, Moscow, 1973) [in Russian].
11. M. A. Zheksenov and A. S. Petrov, J. Commun. Technol. Electron. **59**, 289 (2014).
12. M. A. Zheksenov and A. S. Petrov, J. Commun. Technol. Electron. **59**, 427 (2014).
13. S. E. Bankov, E. M. Guttsait, and A. A. Kurushin, *Solving Optical and Microwave Problems with the Help of HFSS* (Orkada, Moscow, 2012) [in Russian].
14. N. N. Fedorov, *Fundamentals of Electrodynamics* (Vysshaya Shkola, Moscow, 1980) [in Russian].

Translated by E. Chernokozhin